RAPID 3-D RAYTRACING FOR OPTIMAL SEISMIC SURVEY DESIGN

Jie Zhang

Earth Resources Laboratory
Department of Earth, Atmospheric, and Planetary Sciences
Massachusetts Institute of Technology
Cambridge, MA 02139
and
Blackhawk Geometrics, Inc.
Golden, CO 80401

Eugene Lavely

Blackhawk Geometrics, Inc.
Golden, CO 80401

M. Nafi Toksöz

Earth Resources Laboratory
Department of Earth, Atmospheric, and Planetary Sciences
Massachusetts Institute of Technology
Cambridge, MA 02139

ABSTRACT

A useful approach to optimal seismic survey design is to simulate the seismic response for a suite of *a priori* subsurface models and shot-receiver templates. The response can be used to evaluate many criteria such as subsurface coverage, target resolution, noise sensitivity, aquisition footprint, data redundancy, long-wavelength statics resolution, and others. A key requirement for practical implementation is the use of an accurate and rapid simulation method. For most cases survey optimization for a highly detailed 3D model would not be useful because (1) such information is often not available, (2) some of the conclusions may not be robust to small changes in the model, and (3) simulation of generally varying complex models would be prohibitively expensive.

Instead, a more useful model class for survey design would be 3D models with constant velocity layers separated by arbitrary (and possibly complex) interfaces. The models may be from conjecture or previous seismic surveys.

We present a rapid 3D raytracing method optimized for the computation of reflection and refraction wavefronts from a point source in this model class. We demonstrate that the method simulates wave phenomena such as diffraction and head wave propagation. The approach is extremely fast since it avoids traveltime expansion in the volume between interfaces, and solves a simple 2D problem on each interface. Other methods require local propagators (even in constant velocity regions), whereas our approach enables large jumps of wavefronts from interface to interface. The calculation of 3D reflection or refraction traveltimes for a model with an arbitrary interface from one source to any number of receivers requires less than 1 sec of CPU time on a DEC 3000/500 workstation.

We briefly review how our new method can be used to facilitate survey resolution computations. We also develop a method for estimating an efficient source-receiver distribution for resolving an assumed 3D structure. To design the receiver distribution, we calculate continuous traveltime slices at the surface from a given source template and plot the RMS curvatures of the wavefronts. The spatial density of the receiver coverage should be in proportion to the locally-varying magnitude of the RMS curvature. Similarly, to determine the optimal source distribution, we sum the RMS curvatures of the wavefront traveltimes due to each source in the entire survey area. In the same way, the magnitude of the curvatures suggests the most important areas for source locations.

INTRODUCTION

The subsurface resolving capability of a 3-D seismic experiment and the acquisition cost strongly depend on the survey design. In fact, on average, 75% of the costs of a domestic 3-D land survey are in the acquisition stages, 18% in processing and 7% in interpretation. Clearly, an efficient survey design can yield significant acquisition savings, and a data set optimized for the survey objectives will lead to reduced processing costs, improved accuracy of interpretation, and ultimately, increased pay. Therefore, rigorous objective criteria for obtaining optimized 3-D data sets is critical for efficient and economic implementations. Of course, the goals of maximum resolution and minimum exploration cost are generally in conflict, so that survey design is a classic problem in optimization theory beset by trade-offs, uncertainties of assumptions, etc. Another major problem is the identification of the appropriate objective criterion (or criteria) for assessing the utility of a given design. For example, the survey that can best resolve a given horizon may be suboptimal for AVO analysis, or the survey which yields well -resolved migrated images may display poor noise suppression capability. Thus, the choice of the different criterion, their relative weighting, and the computational loads are seen to be basic scientific problems. It is also necessary to weigh the trade-off between objective criterion versus cost of acquisition. Finally, a major practical problem

efficient computation of such criteria. To gain industry acceptance, any survey design work should represent only a small fraction of the total acquisition cost. This requires a rapid and robust design implementation. A brute force method for survey design would be to (1) perform a 3-D finite-difference calculation to generate a synthetic 3-D volume for many source/receiver distributions, (2) run this data through the standard data processing pipeline (including 3-D prestack depth migration), (3) evaluate the objective criteria, and repeat these steps for different designs and earth models. Nevertheless, we seek a more enlightened approach.

The determination of an efficient survey design for a given cost threshold requires several important inputs including an *a priori* reservoir model for seismic response calculation, an objective criterion such as subsurface resolution, and a suite of shot-receiver templates. For the purpose of survey design it is adequate to consider a simplified class of models e.g., constant velocity layers bounded by arbitrary interfaces. We develop a 3-D raytracing method that can rapidly simulate reflection and refraction wavefronts for this model class. The goal is to provide a basic computational tool to facilitate the practical implementation of any number of survey design methods on a PC. Our new ray tracing method is presented in outline in the next section. The method is robust and self-contained so that it can be used in modular fashion in elaborate design optimization processes that require ray tracing results (e.g. Beylkin *et al.*, 1985; Barth and Wunsch, 1990; Lavely *et al.*, 1997). These methods are for decimating shots and receivers in a 3-D survey design without compromising the information content relative to that of a reference survey with a dense distribution of shot-receiver pairs.

RAPID 3-D RAYTRACING METHOD

Simulation of typical 3D surveys would typically require ray path computations for $\mathcal{O}(10^5)$-$\mathcal{O}(10^6)$ source-receiver pairs. Furthermore, this computation will likely need to be repeated for several input seismic models, and certainly for many source-receiver templates. We have chosen the wavefront method to calculate traveltimes and raypaths in our 3-D models since the calculation time is independent of the number of receivers i.e., for a given source, raypaths and traveltimes are computed to all points in the model including all points on the surface. Existing 3-D wavefront methods include finite-difference approximations to the eikonal solution (e.g., Vidale, 1990; Hole and Zelt, 1995) and the shortest path methods by Saito (1990) and Klimes and Kvasnicka (1993). The later methods follows from the 2-D approaches of Saito (1989) and Moser (1989, 1991). These methods can be used to calculate traveltimes to all grid points in complex velocity models. However, they do not provide computational savings when the input models are simplified to the model class considered here (i.e. constant velocity layers bounded by complex interfaces). This is because the solution of the eikonal equation with a finite-difference method is a *local* approach i.e., it must expand a local square wavefront progressively and cannot make large spatial jumps. The shortest path method requires expansion along a virtual wavefront, and as with the finite-difference

method, cannot make large spatial jumps. The method that we present in what follows is uniquely suited for the restricted class of velocity models that we consider. In essence, it combines Snell's law with graph theory to expand directly wavefronts from one interface to another in a 3-D model.

The 3-D seismic model is gridded in horizontal directions (x and y) only. In the z dimension, the internal interfaces and the surface topography are defined as depth functions $d(i,j)$ where the independent variables i and j are the grid coordinates for each interface. The functions $d(i,j)$ may adopt any real value. This model representation results in significant savings in the numerical implementation since 3-D volumes of data need not be stored. Instead we need only store a few 2-D vectors that define the interface topography, and 2-D traveltime and raypath vectors for each interface.

For the one interface problem, the method consists of the following steps:

1. Find any hidden areas on the interface that cannot be reached by straight rays from the source, and then compute 2-D traveltime vectors from the source to each grid point in the nonhidden areas using the straight rays.

2. If a refraction calculation is required, a directional graph template is applied to find the shortest path connection on the interface, and then the refraction times are accounted for.

3. Propagate the wavefront from the interface back to surface, using Snell's law to estimate up-going ray coverage for determining the size of a square graph template.

For the multiple interface problem, the propagator from interface to interface as established in step (3) can be used repeatedly to map traveltimes and raypaths from one interface to another either downward or upward.

The first step is not necessarily required for all models. However, hidden areas may occur when the interface has large depth variations. Detection of the hidden areas is important since raypaths in their vicinity may be complicated, and since diffractions may be generated from their edges. In practice, we seek the diffraction points first and then determine the areas which are hidden behind the diffractors. When the angle between the vector of an incident ray and the normal vector of a reflector is less than 90°, the local reflector must be hidden from the source, i.e.,

$$\cos\theta = \frac{\vec{n}\cdot\vec{p}}{|\vec{p}|} < 0 \longrightarrow hidden\ reflector \tag{1}$$

where $\vec{n}$ is the normal vector of a reflector, and $\vec{p}$ is a vector of the incident ray. Figures 1a defines the notation. The simple vector operation in equation (1) efficiently defines the location of diffraction points. At the same time we store $\vec{n}$ for further calculations. However, the above rule can only help us to find some of the hidden reflectors. After those of the reflectors satisfying the above rule are found, a directional graph template is applied to search others in vicinity which do not satisfy the above rule but are hidden behind those just found. That is, we seek to determine if any segment of the straight

ray path connection between the source and the node is under the interface. Figure 1b shows the shape of a graph template. Following the direction from the source location to the diffraction point, a graph template extends its coverage until no more hidden points are found. After all hidden points are found, their times $t(i,j)$ are assigned a very large default value, and all remaining points are timed with straight rays from the source. In performing seismic traveltime calculations with graph theory, a graph template is used to select nodes for updating traveltimes (Saito, 1989, 1991; Moser, 1989, 1990). However, here we apply a variable graph template to select nodes for finding hidden areas. This approach allows us to deal with nodes, uniformly, automatically and efficiently. We will show later that other graph templates are also designed at different stages in this rapid raytracing calculation. We apply the graph templates on the interfaces, and the template is three-dimensional for non-planar interfaces. However, from the plan view, it is a 2-D problem, and indeed, we only need to solve a 2-D problem.

If a refraction computation is required, we continue to work on the interface and apply another graph template to find the critical refraction points and their connections with other nodes. This turns out to be extremely simple with a graph template. Figure 2 illustrates a graph template with a fixed number of nodes but variable shapes at different locations. At each point on the interface, we use this graph template to update the times from a master point if necessary. Assuming that the time at the master point (n,m) is $t(n,m)$ and the minimum time between the master point and the current working node (i,j) on the template is t_r, we apply the following algorithm:

for any point (i,j) on the graph template:
if $[t(n,m) + t_r < t(i,j)]$ then
(1) $t(i,j) = t(n,m) + t_r$
(2) $ipath(i,j) = n + (m-1)nx$
endif

where $ipath(i,j)$ is a vector for storing raypaths, $t(i,j)$ may be a direct traveltime from the source or updated refraction time from other master point. Because we search for a minimum-time connection from all possible neighbors using a graph template, the algorithm does not require that we order the nodes in any particular way. Therefore, we loop over all nodes on the interface without the need for sorting, and this represents a significant cost savings. This approach differs from the shortest path raytracing algorithms (Saito, 1989, 1990; Moser, 1989, 1991) since these require the application of the graph template along the virtual wavefront. After applying the above algorithm we can track raypaths using the computed quantity $ipath(i,j)$ and integrate refraction times on the interface and the time from the source to point (i,j). The result updates $t(i,j)$.

The third step is required for both reflection and refraction calculations. Wavefronts from both ray types need to propagate back to the surface from the interface. In fact, mapping wavefront traveltimes from one interface to another and ultimately to the surface is the primary concern of this study. First, nodes at the surface of the model

are assigned with a very large default value for reflection calculations, or with direct traveltimes for refraction calculations. We apply Snell's law to determine the directions of rays propagating upwards from the interface. For this purpose, vector operations are efficient and reliable. We denote an up-going ray vector by $\vec{q}$. To determine $\vec{q}$, we must consider three different cases:

(1) reflection: $\vec{q} = \vec{p} - 2(\vec{p} \cdot \vec{n})\vec{n}$
(2) refraction: $\vec{q} = |\vec{p}| \cos\beta \ \vec{n} + \sin\beta \ \vec{p}$
(3) transmission: $\vec{q} = |\vec{p}|(\cos\beta - \sin\alpha\cos\alpha\sin\beta) \ \vec{n} + \sin\alpha\sin\beta \ \vec{p}$

where α is the incident angle beneath the interface, and β is the angle between $\vec{q}$ and $\vec{n}$. We have assumed that $|\vec{q}| = |\vec{p}|$. In the above formulation the amplitude is immaterial, and only the vector direction is required in the calculation. Formulas (2) and (3) above are for the case of refraction. Transmission from the lower to the upper medium occurs when the angle of the refracted ray propagating upwards from the lower medium is less than 90°. The angles α and β can be determined from the following relationships:

$$\cos\alpha = \frac{\vec{p} \cdot \vec{n}}{|\vec{p}|} \tag{2}$$

$$\sin\beta = \frac{v_1}{v_2} \sin\alpha \tag{3}$$

where v_1 and v_2 are the velocities in the upper and lower medium, respectively.

Using the above algorithms, we first calculate $\vec{q}$ for every point on the interface. As shown in Figure 3, the graph template size and location at the surface for each point on the interface are determined by the ray directions of its four neighbor nodes. If the computed location of a graph template is not contained within the surface of the model, the default of the graph template is placed at the surface following $\vec{q}$ to calculate any possible diffraction.

The above three-step approach is robust and efficient. It is sophisticated enough to deal with complex interface shapes. We design three different graph templates that can optimize the calculation in three steps. The approach is computationally efficient since it is not necessary to perform a wavefront expansion within the 3-D volumes bounded by the internal interfaces. Figure 4 demonstrates a numerical example in which we compute the traveltimes of a reflected wavefront for a dome model. The results clearly illustrate that both wave phenomena (diffraction) and ray phenomena (reflection) are modeled. Figure 5 shows a refraction calculation for a fault model. The diffraction effect from the edge of the fault is clearly evident in this example as well. The computations in Figures 4 and 5 each required less than 1 sec of CPU time on a 160 MHz DEC-Alpha workstation.

OPTIMAL SEISMIC SURVEY DESIGN

The computational efficiency demonstrated in the previous section is an important advance since it makes optimized survey design computationally feasible. For a 3-D numerical model that is constructed from an *a priori* seismic model, we can calculate wavefront traveltimes for thousands of shots in less than 15 minutes of CPU time on our 160 MHz DEC-Alpha workstation. There are a number of ways to evaluate the utility of survey designs. First, we describe methods based on inverse theory, and then present a method that may be used to estimate how a survey may be decimated without compromising the data control on the subsurface structure. These methods strongly rely on ray tracing results, but are clearly impractical without the availability of a rapid, robust, and accurate ray tracer. Of course, for smaller scale problems, computation time is less of a concern. For example, Barth and Wunsch (1990) computed the optimal experimental deployment of sources and hydrophones for an ocean acoustic tomographic experiment. They confined their attention to a total of nine sources and receivers and the objective criterion they chose was to maximize the smallest singular value of the design matrix. They searched the experiment parameter space using a simulated annealing algorithm. They applied a global optimization technique, but their problem was nonetheless tractable due to the limited parameter space, and the simplified physics of ocean acoustic wave propagation. In our problem, wave propagation will typically be much more complex, and the parameter space to be explored is vastly larger. Issues of global optimization for 3-D surveys deserve study. However, in preface to this, it will be helpful to simply restrict the parameter space, and evaluate the relative merits and trade-offs of a limited set of designs.

Use of Inverse Theory for Improved Survey Design

A qualitative approach to the analysis of acquisition geometry using, for example, visualization of ray paths to ensure adequate bin coverage, can provide useful insights, but the results are difficult to quantify. On the other hand, we can draw on the results of inversion theory to obtain a more quantitative result. In fact, inverse theory can provide a powerful framework for survey design optimization. Inverse methods may broadly be classified into either (1) operator-based approaches such as migration, or (2) model-based approaches such as traveltime tomography. In conventional inversions, experimental design parameters are assumed fixed, and data are inverted for the desired model. In design optimization, the experiment parameters are adjusted until a data set that will yield a model solution with the desired properties is obtained. These may include maximum model resolution, minimum model covariance, robustness to noise, and many others. Operator-based inversion methods estimate model parameters directly from the observed data using a specified mathematical model for wave propagation. Layer-stripping inversion, and migration are examples of operator-based inversion.

An example of operator-based inversion for improved survey design is given by Gibson *et al.* (1994). They performed a modeling study to design a source configuration

which could be used to collect VSP data suitable for 3-D elastic wave Kirchoff migration. Synthetic seismograms were computed for a variety of source configurations over a model of deep reflectors below the known shallow geology of the site. They then applied Kirchoff migration to these results, and were thereby able to assess the imaging potential of possible future field experiments at the site.

An example of model-based inversion for improved survey design is given by Barth and Wunsch (1990) in the ocean acoustic experiment described above. Their goal was to resolve as well as possible the slowness values of voxels within a regular grid. In general, the appropriate objective criterion depend on the goals of the survey, but they showed that many desirable solution properties may be achieved for surveys in which the design matrix G has a condition number as near as possible to unity. Another way of stating this is that the smallest singular value of G should be as large as possible. In their case, the inverse problem was given by $G\ m = d$ where m are the desired slowness values and d is the data. They perturbed the source and receiver distribution using simulated annealing until their objective function (the smallest singular value) was maximized.

We note that the studies of Gibson *et al.*(1994) and Barth and Wunsch (1990) both required raytracing, and this was by far the most intensive computational element of their programs.

Inverse Theory and Survey Design Based on Generalized Radon Transform

Beylkin (1985) and Beylkin *et al.* (1985) presented a general approach to the description of the spatial resolution of seismic experiments and migration (or inversion) algorithms. They considered the inverse scattering problem for the Helmholtz equation which governs acoustic wave propagation. The theory allows for an arbitrary background medium and arbitrary configuration of sources and receivers. They showed that the spatial resolution of a given point can be defined by the domain of coverage in the spatial wavenumber domain. This domain depends on a mapping into spatial wavenumber space of the frequency band of the signal, and a functional that is dependent on the source-receiver configuration and on the background medium. Their detailed development reduces to a remarkably simple and intuitive result. Suppose the scatterer is described in object space by the function $f(\boldsymbol{x})$ and that its Fourier transform is $\hat{f}(\boldsymbol{k})$ where $\boldsymbol{k}$ is the spatial wavenumber vector. Beylkin *et al.* find that an estimate $f_{est}(\boldsymbol{x})$ of f is given by

$$f_{est}(\boldsymbol{x}) = \frac{1}{(2\pi)^3} \int_{D_{\boldsymbol{x}}} \hat{f}(\boldsymbol{k}) e^{-\boldsymbol{k}\cdot\boldsymbol{x}} d\boldsymbol{k}. \tag{4}$$

The description of the domain of integration D_x is, in fact, the estimate of spatial resolution. For a given point $\boldsymbol{x}$ in the medium, this description is given by the mapping

$$\boldsymbol{k} = \omega[\nabla\tau(\boldsymbol{x}, \boldsymbol{s}) + \nabla\tau(\boldsymbol{x}, \boldsymbol{r})]. \tag{5}$$

This mapping is of fundamental importance for survey design since the domain of integration $D_{\boldsymbol{x}}$ in equation (4) is defined by this expression for $\boldsymbol{k}$. Here, ω is the frequency,

x is the imaging point, s is the source location, r is the receiver location, $\nabla\tau(x,s)$ is the slowness vector at the imaging point connecting the source with that point, and $\nabla\tau(x,r)$ is the slowness vector connecting the imaging point with the receiver. The sum of the slowness vector terms defines a vector that bisects the angle defined by the ray segments. This defines the direction of the wavenumber vector that can be recovered for this particular source-receiver pair. The result in equation (5) defines the resolution of seismic imaging for a given experiment.

It is important to realize that the above results comes from a solution to the seismic inverse problem using the Generalized Radon Transform. In most inverse problems it is only possible to estimate resolution by actually inverting a matrix (e.g., Barth and Wunsch, 1990) which can be numerically intensive and unstable. Here, however, we are able to estimate resolution by performing forward ray tracing computations. This is a powerful advantage for the routine and practical use of this method, especially with the availability of a rapid 3-D ray tracer. Lavely *et al.* (1997) used the results in equations (4) and (5) to develop simple and intuitive methods of evaluating competing survey designs. They concentrated on the effect of limited aperture on coverage in the spatial wavenumber domain. The recovery without distortion of a point scatterer in object space would, in general, require complete source-receiver coverage on a surface such as a sphere that encloses the point. In addition, all frequencies are required, the background model must be perfectly known, and all unmodeled wave phenomena should be accounted for or filtered from the data. If all of these conditions were met but only limited signal bandwidth is available, then instead of a point image, we would recover a finite size object with half-width determined by the finite frequency bandwidth. In reality none of the above conditions are met and so we only recover a distorted and band-passed image of the object.

Method for Decimating Surveys

We present a method to estimate a deployment of sources and receivers that accounts for the spatially varying rate of seismic data. The principal idea is that regions with high data curvatures should have dense coverage so that important structural information can be resolved, whereas regions with low data curvatures should have sparser coverage so that acquisition costs can be reduced. Thus, the goal is to decimate surveys in regions where variations are linear or smooth so that loss of independent data information is minimized, and to oversample selected regions so that required resolution can be achieved.

The approach we use is straightforward. First, we compute reflection and/or refraction wavefronts for a fixed subsurface model (as defined earlier). We then use the computed traveltimes for further analysis. The above computation is performed for a finite number of sources but with an extremely dense receiver distribution. The high density receiver distribution is used so that we may calculate "continuous" traveltime slices on the surface. This yields a data set with maximum information content, which can be used as the reference data set so that the effects of decimation may be eval-

uated later. We then compute two functionals from the traveltime results, the RMS receiver-time curvature and the source-time curvature. The first functional measures the complexity of wavefront traveltime variation to every point in the survey field from all shots. The second functional measures the complexity of wavefront traveltime variation to all receivers from each shot. We use these functionals to determine a decimated source and receiver distribution that meets the resolution requirement of the survey, but at reduced cost.

To measure the complexity of a traveltime slice, we calculate the spatial curvature of the traveltimes using a Laplacian operator. We accumulate the traveltime curvatures from n surface sources and define a functional of the RMS receiver-time curvatures for the entire survey area:

$$c_r(x,y) = \sqrt{\frac{1}{n}\sum_{i=1}^{n}\left(\frac{\partial^2 T_i}{\partial^2 x} + \frac{\partial^2 T_i}{\partial^2 y}\right)^2} \tag{6}$$

where T_i is the traveltime slice due to ith source, and the derivatives are evaluated at the receiver locations (x,y). The functional $c_r(x,y)$ is a local quantity whose value at a given receiver is dependent on the source distribution but independent of the receiver distribution. Thus, for a given source distribution, $c_r(x,y)$ can be used to design an optimal receiver layout. For example, a relatively large value of c_r at point (x,y) suggests there may be large traveltime variations in this vicinity, and therefore, a dense receiver distribution there would be advisable. We note that survey design conclusions are simplified by the fact that only the relative magnitude of the functional is relevant.

We now consider source distribution optimization for a survey with a fixed number of receivers. To do this, we define a functional of the RMS source-time curvatures:

$$c_s(x_i,y_i) = \sqrt{(\sum_{j=1}^{m}(\frac{\partial^2 T_i}{\partial^2 x_j} + \frac{\partial^2 T_i}{\partial^2 y_j})^2)/m} \tag{7}$$

where again j is the receiver index, m is the total number of receivers, (x_j,y_j) is the jth receiver location, and the derivatives of T_i from source i are evaluated at the receiver locations (x_j,y_j). The above functional simply sums the traveltime curvatures at all the receiver points due to a single shot located at (x_i,y_i). Therefore, $c_s(x_i,y_i)$ depends on the entire receiver distribution, but is independent of the other shot distribution. The calculation in equation (7) is repeated for all possible shot locations. For a fixed receiver template, a 2D contour of the resulting function $c_s(x_i,y_i)$ can then be used to design an optimal source distribution. If $c_s(x_i,y_i)$ is relatively large, it suggests that there should be a high density of shots in the vicinity of (x_i,y_i), or at least that selected shots there will be important for generating significant features in the recordings. Thus, one can use the relative magnitudes of $c_s(x_i,y_i)$ to define a non-uniform source distribution that will increase resolution and decrease costs. Costs can be decreased by decimating the shot distribution in regions of relatively low $c_s(x_i,y_i)$ values.

In Figure 6, we provide a numerical example using the above approaches to survey optimization. Figures 6a and 6b show a dome model with a constant overburden velocity of 1000 m/s. We calculate the functionals in equations (6) and (7) for two different cases. In the first case, we assume that the sources and receivers for a reflection survey are confined to a square surface area of 200×200 (m^2). We uniformly populate the survey grid with sources in 4 m increments in both the x and y directions for a total of 2500 sources. We then compute traveltimes for all of these sources to a set of receiver locations that are coincident with the source locations. The total calculation takes about 18 min on a DEC 3000/500 workstation. It is important to note that the CPU time for the wavefront method is independent of the number of receivers. In the second case, we assume there is a square exclusion zone in which sources and receivers may not be deployed. This reduces to 1900 the total number of shots.

Figure 6c shows the contour of the RMS receiver-time curvatures with the highest magnitude in the central circle for the first case. This calculation assumes that a source template with 50×50 shot points has been selected, and that one wishes to understand how receivers should be distributed for effective coverage. The figure shows that for the case of uniformly distributed shots, the most important receiver locations are near the top of the dome. Figure 6d illustrates the functional of the RMS source-time curvatures. This figure can be used to determine the most effective source locations. It suggests that these locations start from the central area and progressively expand outward. This conclusion is for the case in which receivers are uniformly distributed through the square survey field.

In a real field survey there will be numerous culturally sensitive areas in which sources or both sources and receivers must be excluded. The method we have developed is capable of handling arbitrarily shaped exclusion zones. Figures 6e and 6f shows an example of an exclusion zone in the upper-right corner of the survey. Therefore, we calculate the functionals in equations (6) and (7) in the remaining area. If sources are uniformly distributed in the available region we observe that the important locations for deploying receivers start from the top of the target and expand outward and also slightly downward as shown in Figure 6e. On the other hand, if receivers are uniformly distributed in the open field, Figure 6f shows that the important source locations start from the central contour and expand over a slightly larger area along an axis between the upper-left and the lower-right corners.

The approach we described is flexible since it can be used for any source-receiver template. One can rapidly explore many variations of the survey parameters and assess the effectiveness of each combination. Because of its extremely high efficiency, the approach can be also in a near real-time basis during field operations to improve survey design. For example, after receivers are deployed and a few shots are detonated, one can replace some of the synthetic traveltimes with real data and repeat the calculation of the curvature functionals to improve the estimate. It is also important to note that the approach evaluates the continuity of wavefronts in 3D media and honors many wave effects. The absolute traveltimes from an *a priori* model may not be reliable, and are

avoided in the functionals for survey design. The design approach is robust and requires minimal input from the user, only an assumed source template for determining receiver locations, an assumed receiver template for determining source locations, and an *a priori* subsurface model. These requirements are not unreasonable.

CONCLUSIONS

We developed a rapid 3-D raytracing method for calculating wavefront traveltimes in simplified Earth models. Unlike conventional wavefront approaches, this method maps wavefronts directly from one interface to another i.e., it does not require incremental updating or spatial expansion within the constant velocity layers that define the seismic model. Therefore, the method is extremely fast, and brings the computationally intensive effort of optimal seismic survey design a step closer to practical implementation. The method can serve as a computational module for numerous design methods. We described some of these approaches, and introduced a new design method as well. The method involves estimating resolution capability by calculating RMS residuals between one shot record and others. The speed of this approach presents the opportunity to make near real-time decisions in the field for routine use.

ACKNOWLEDGMENTS

The authors gratefully acknowledge the Gas Research Institute for support of this research for the Gas Research Institute for Advanced Seismic Data Acquisition and Processing under Contract # 5096-210-3781. We also thank Dr. Timothy Fasnacht, our program manager at GRI, for advice and feedback. This work was also supported by the Reservoir Delineation Consortium at the Massachusetts Institute of Technology.

REFERENCES

Barth, N. H. and Wunsch, C., 1990, Oceanographic experiment design by simulated annealing, *J. Phys. Ocean., 20*, 1249-1263.

Beylkin, G., 1985, Imaging of discontinuities in the inverse scattering problem by inversion of a causal generalized Radon transform. *J. Math. Phys., 26*, 99-108.

Beylkin, G., Oristaglio, M. and Miller, D., 1985, Spatial resolution of migration algorithms, in Berkhout, A.J., RIdder, J., and van der Wall, L.F., eds., *Acoustical Imaging, 14*, Pleum Press, New York, pp. 155-167.

Gibson, Jr., R.L., Lee, J.M., Toksöz, M.N., Dini, I. and Cameli, G.M., 1994, The application of 3D Kirchoff migration to VSP data from complex geological settings, 63rd Ann. Internat. Mtg. Soc. Explo. Geophys. Expanded Abstracts, 1290-1293.

Hole, J. A. and Zelt, B. C., 1995, 3-D finite-difference reflection traveltimes, *Geophys. J. Int., 121,* 427-434.

Klimes, L. and Kvasnicka, M., 1993, 3-D network ray tracing, *Geophys. J. Int., 116*, 726-738.

Lavely, E. M., Gibson, Jr., R. L. and Tzimeas, C., 1997, 3D seismic survey design for optimal resolution, submitted to SEG Expanded Abstracts for Fall, 1997 meeting.

Moser, T. J., 1989, Efficient seismic ray tracing using graph theory, Soc. Exploration Geophys. 1989 Meeting, Expanded Abstracts, SEG, Tulsa, OK, 1106-1031.

Moser, T. J., 1991, Shortest path calculation of seismic rays, *Geophysics, 56*, 59-67.

Saito, H., 1989, Traveltimes and raypaths of first arrival seismic waves: computation method based upon Huygens' principle, Soc. Exploration Geophys. 1989 Meeting, Expanded Abstracts, SEG, Tulsa, OK, 244–247.

Saito, H., 1990, 3-D ray tracing method based on Huygens' principle, Soc. Exploration Geophys. 1990 Meeting, Expanded Ebstracts, SEG, Tulsa, OK, 1024-1027.

Vidale, J., 1990, Finite-difference calculation of traveltimes in three dimensions, *Geophysics, 55,* 521-526.

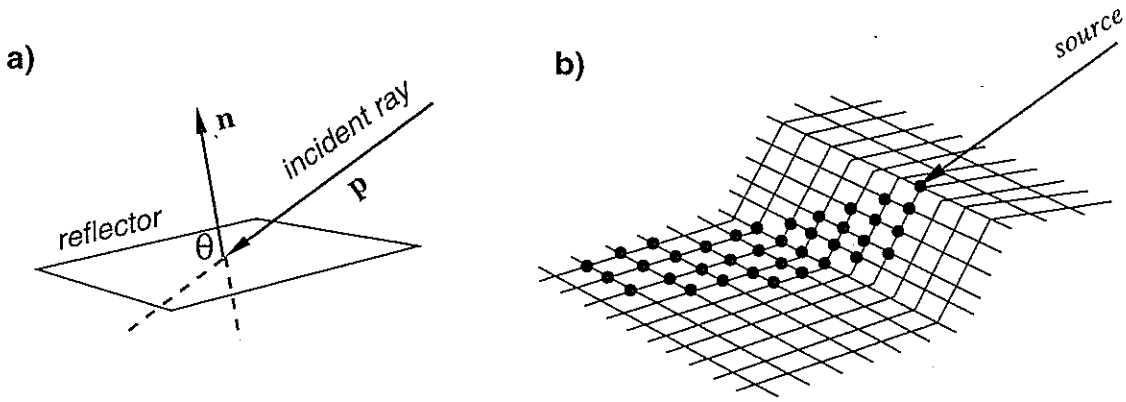

Figure 1: (a) Notation of a normal vector for a reflector, incident ray and their angle. (b) Graph template to determine hidden nodes behind a diffraction point. The search starts from the diffraction point and extends away from the source direction until no hidden points are found.

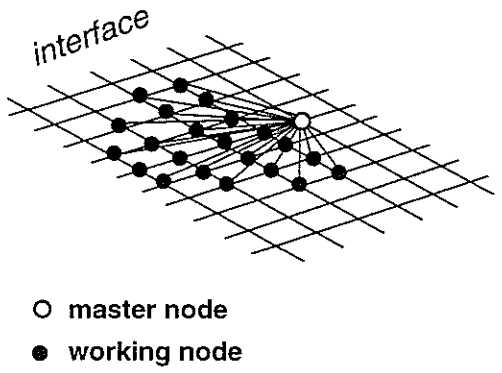

Figure 2: Refraction graph template on an interface. The number of working nodes is fixed for each master node, but the template shape varies according to its relative lolcation to source point.

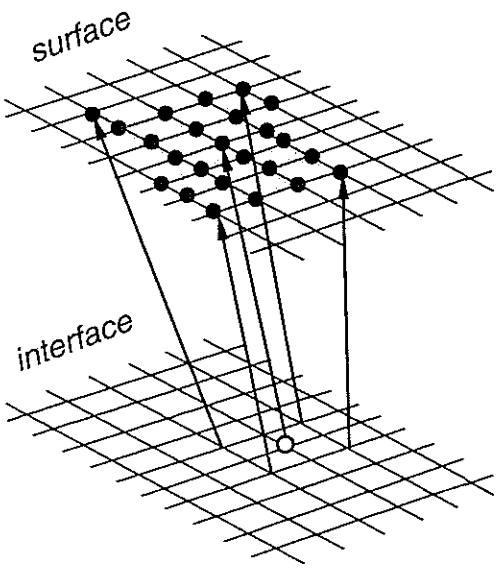

Figure 3: Graph template on the surface for mapping up-going wavefront traveltimes. The size and shape of the template are determined by the up-going rays from the master node on the interface and also from its four neighbor nodes.

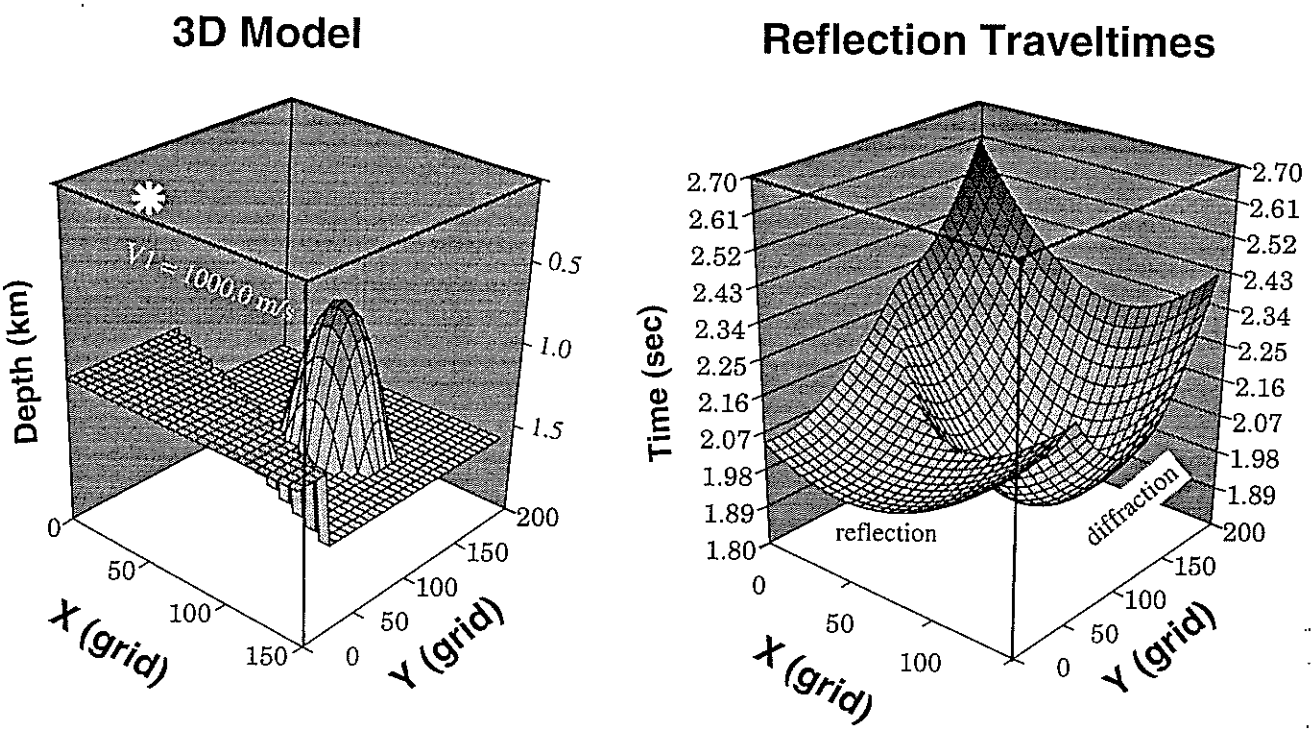

Figure 4: Numerical model consisting of a fault and a dome. The reflection wavefront from a source is calculated.

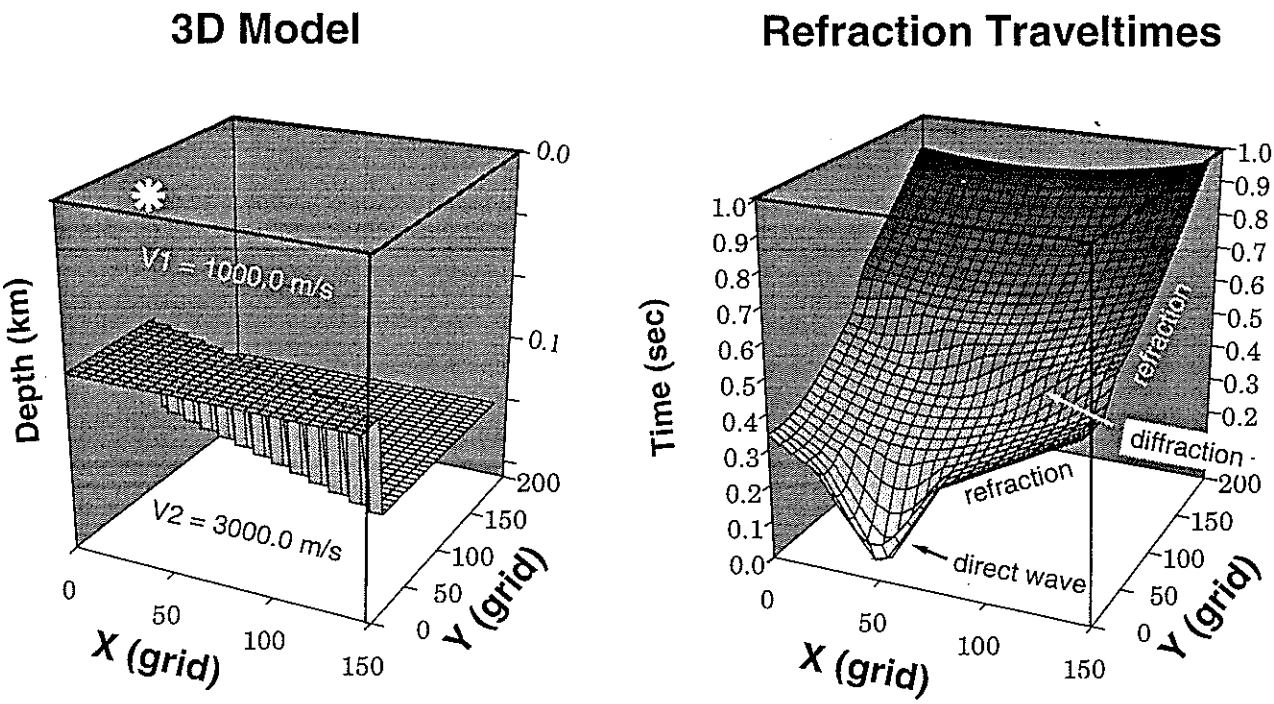

Figure 5: Numerical model consisting of a fault. The refraction wavefront from a source is calculated.

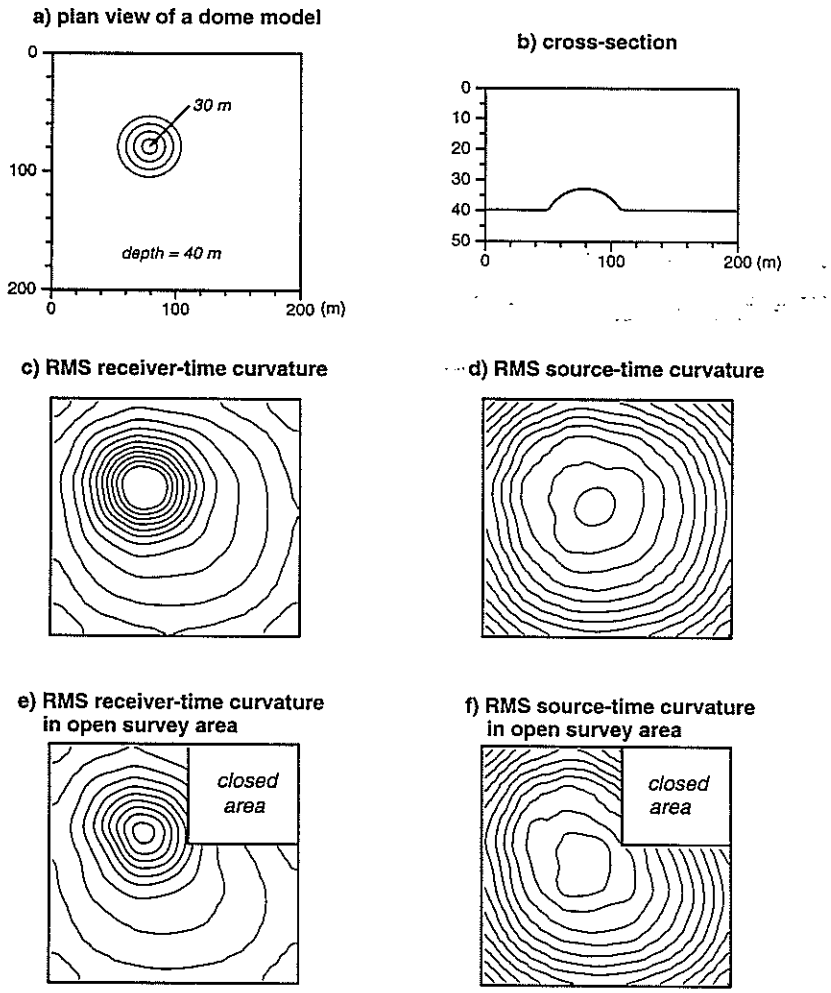

Figure 6: Numerical simulation for optimal survey design. (a) Plan view of a dome model. (b) Cross-section of the model. (c) Distribution of RMS receiver-time curvatures (see text for definition) when the sources are uniformly placed in the survey area, the central contour represents the highest magnitude. (d) Distribution of RMS source-time curvatures (see text for definition) when the receivers are uniformly placed in the survey area, the central contour represents the highest magnitude. (e) Distribution of RMS receiver-time curvatures when a small area is not available for survey. (f) Distribution of RMS source-time curvatures when a small area is not available for survey.